Electrical properties of resistive switches based on $Ba_{1-x}Sr_xTiO3$ thin films prepared by RF co-sputtering

A. Márquez-Herrera,[a,b] E. Hernández-Rodríguez,[a] M.P. Cruz,[c] O. Calzadilla-Amaya,[d] M. Meléndez-Lira,[e]
J. Guillén-Rodríguez,[b] and M. Zapata-Torres[a]

[a]*Centro de Investigación en Ciencia Aplicada y Tecnología Avanzada,*
Unidad Legaria IPN, Calzada Legaria 694, Col. Irrigación, México D.F., 11500 México,
e-mail: amarquez@ipn.mx
[b]*Instituto Tecnológico y de Estudios Superiores de Monterrey, Campus Tampico,*
Puerto Industrial, Altamira, Tamaulipas, 89600, México.
[c]*Universidad Nacional Autónoma de México, Centro de Nanociencias y Nanotecnologia,*
Km. 107 Carretera Tijuana-Ensenada, 22860, Ensenada, B.C. México.
[d]*Facultad de Física-IMRE,*
Universidad de la Habana, Cuba.
[e]*Departamento de Física, Centro de Investigación y de Estudios Avanzados del Instituto Politécnico Nacional,*
Apartado Postal 14-740, México D.F., 07000 México.

In this work, we propose the use of $Ba_{1-x}Sr_xTiO_3 (0 \leq x \leq 1)$ thin films for the construction of MIM (metal-insulator-metal) heterostructures; and their great potential for the development of non-volatile resistance memories (ReRAM) is shown. The deposition of $Ba_{1-x}Sr_xTiO_3$ thin films was done by the rf co-sputtering technique using two magnetron sputtering cathodes with $BaTiO_3$ and $SrTiO_3$ targets. The chemical composition (x parameter) in the deposited $Ba_{1-x}Sr_xTiO_3$ thin films was varied through the rf power applied to the targets. The constructed MIM heterostructures were Al/$Ba_{1-x}Sr_xTiO_3$/nichrome. The I-V measurements of the heterostructures showed that their hysteretic characteristics change depending on the Ba/Sr ratio of the $Ba_{1-x}Sr_xTiO_3$ thin films; the Ba/Sr ratio was determined by employing the energy dispersive spectroscopy; SEM micrographs showed that $Ba_{1-x}Sr_xTiO_3$ thin films were uniform without cracks or pinholes. Additionally, the analysis of the x-ray diffraction results indicated the substitutional incorporation of Sr into the $BaTiO_3$ lattice and the obtainment of crystalline films for the entire range of the x values.

Keywords: Barium strontium titanate; thin films; non-volatile memories; ReRAM cells.

En este trabajo, se propone el uso de películas delgadas de $Ba_{1-x}Sr_xTiO_3 (0 \leq x \leq 1)$ para la construcción de heteroestructuras metal-aislante-metal (MIM por sus siglas en inglés) y se muestra el gran potencial que poseen para el desarrollo de memorias no volátiles resistivas (ReRAM). El depósito de las películas de $Ba_{1-x}Sr_xTiO_3$ se hizo mediante de la técnica de rf-sputtering usando dos cañones tipo magnetrón con blancos de $BaTiO_3$ y $SrTiO_3$, respectivamente. La composición química de las películas (parámetro x) fue variado a través de la potencia aplicada a cada uno de los blancos. Las heteroestructuras depositadas fueron Al/$Ba_{1-x}Sr_xTiO_3$/nichromel. Las pruebas I-V de las heteroestructuras mostraron que es posible cambiar su comportamiento eléctrico mediante la variación de la proporción Ba/Sr presente la película de $Ba_{1-x}Sr_xTiO_3$; la proporción Ba/Sr fue determinada por espectroscopia de energía dispersada. Las micrografías obtenidas mediante un microscopio electrónico de barrido mostraron que las películas son uniformes y no presentan fracturas ni huecos. Por otra parte, la caracterización de las películas por difracción de rayos x mostró la incorporación sustitucional del Sr en la red del $BaTiO_3$ y la obtención de películas cristalinas para todo el intervalo de valores de x.

Descriptores: Titanato de bario y estroncio; películas delgadas; memorias no volátiles; memorias ReRAM

1. Introduction

The novel properties of ferroelectric thin films for applications in microelectronics, have increased the research activities on these materials in recent years. The $Ba_{1-x}Sr_xTiO_3$ (BST) compound has inspired great interest because it combines the ferroelectric characteristics of the $BaTiO_3$ (BTO) and the mechanical stability of the $SrTiO_3$ (STO). It has been shown that the ferroelectric properties of this material can be modified changing the Ba/Sr ratio [1], openning the possibility for a wide range of applications from simple capacitors to ferroelectric nonvolatile memories (FeRAM) [2-8]. Recently, resistive random access memories (ReRAM) have attracted much attention as nonvolatile memories. A ReRAM memory cell is composed of two metallic electrodes separated by a functional insulator (MIM structure). This device can exhibit two or more different ohmic resistances referred in the simplest case as high resistance state (HRS) and low resistance state (LRS). The resistance states are permanent and can be toggled between them easily exceeding threshold voltages V_{SET} or V_{RESET}. The LRS and the HRS states are the experimental implementation necessary for a binary processing of the information. The state of the device is retrieved by measuring the electrical current, when a small voltage V_{READ} is applied. ReRAM memories play an important role in the development of non-volatile memories with improved characteristics because they have higher re-

tention properties, non-destructive extraction of information, low power consumption energy, high operating speed and; especially, because of its multi-dimensional structure that enables the construction of ultra high-density memories [9].

Although it is found that the compound BST has good and stable electrical properties for its application in ferroelectric devices, there isn't any study related to its use in ReRAM memories yet. This paper discusses the electrical properties of Al/$Ba_{1-x}Sr_xTiO_3$/nichrome MIM structures and their relation with the structural properties and chemical composition of the $Ba_{1-x}Sr_xTiO_3$ thin films.

The Al/$Ba_{1-x}Sr_xTiO_3$/nichrome heterostructures were prepared to evaluate the dependence of their resistive switching properties on the chemical composition and structure of the BST films. The BST thin films, with $0 \leq x \leq 1$, were prepared by rf co-sputtering technique using two 2-inch diameter magnetron sputtering cathodes, employing STO and BTO targets with a purity of 99.95%.

2. Experimental details

To prepare the BST thin films, the sputtering chamber was evacuated to a pressure of 1.2×10^{-3} pascals or less, then a "flushing" was performed with argon gas at a pressure of 3.9 pascals during 10 minutes. For the deposition, an Ar + O_2 gas mixture was introduced in the chamber with a ratio Ar/O_2 = 90/10 at a pressure of 6.6 pascals to ignite the plasma and do a pre-sputtering to the target for a time of 15 minutes. Finally, the working pressure was kept at 3.9 pascals to carry out the deposition. The substrate was rotated at 100 rev/min to promote the film uniformity and was heated to 495°C to crystallize the films *in-situ* [10]. To reduce the re-sputtering caused by the negative oxygen ions, the off-axis geometry was employed with an angle of 30° between the targets and the substrate; the presence of O ions in Ar + O_2 sputtering atmospheres is well known and has already been reported by several authors [11-13]. The deposition time was modified in each run to obtain a thickness of 240 nm for all the samples. The BST films were deposited on nichrome substrates using a commercial strip of nichrome 80 with a 0.127 mm thickness produced by the H. Cross company. The reasons for the use of this material have already been published [14,15]. Patterned Al top electrodes with diameter of 1mm were formed by thermal evaporation employing a metallic mask. A distance of 30 mm between the evaporation source and the substrate holder was used; a deposition time of 2 minutes produced electrodes with 0.1 mm thickness.

The thickness of the deposited films was measured using a Dektak3ST profiler by Veeco Instruments.

The microstructure and chemical composition were analyzed with a scanning electron microscope (SEM) Jeol JSM-5300 equipped with a Kevex energy dispersive spectrometer (EDS) model Delta 1. The X-ray diffraction (XRD) spectra of the films were obtained by a Philips X'pert spectrometer using the CuK$_\alpha$ line ($\lambda_{\alpha k1}$=1.54056 Å and $k_{\alpha y \lambda}$=1.54439 Å).

TABLE I. RF-power applied to each sputtering cathode to obtain $Ba_{1-x}Sr_xTiO_3$ thin films with different chemical compositions.

Sample	BTO Power (W)	STO Power (W)
BTO	120	0
BTO105	105	15
BTO90	90	30
BTO75	75	45
BTO60	60	60
BTO45	45	75
BTO30	30	90
BTO15	15	105
STO	0	120

TABLE II. Atomic percentage of the elements on the $Ba_{1-x}Sr_xTiO_3$ films as obtained from EDS measurements.

Sample	Ba	Sr	Ti	O
BTO	18.79 ±0.94	0	21.92 ±1.09	59.29 ±2.96
BTO105	21.25 ±1.06	0.27 ±0.01	23.27 ±1.16	55.21 ±2.76
BTO90	18.83 ±0.94	1.21 ±0.06	23.05 ±1.15	56.91 ±2.84
BTO75	16.68 ±0.86	3.93 ±0.20	21.54 ±1.08	57.85 ±2.89
BTO60	12.10 ±0.61	6.72 ±0.34	20.20 ±1.01	60.97 ±3.05
BTO45	7.43 ±0.37	9.62 ±0.48	18.96 ±0.95	63.99 ±3.20
BTO30	5.06 ±0.25	14.55 ±0.73	18.40 ±0.92	61.99 ±3.10
BTO15	0.13 ±0.01	19.93 ±1.00	19.25 ±1.06	60.68 ±3.03
STO	0	18.66 ±0.93	18.77 ±0.96	62.57 ±3.13

3. Results and discussion

To produce BST films with different chemical compositions, the rf-power applied to the targets was varied in the growth of each film, as shown in Table I.

Figure 1 displays the SEM images of the $Ba_{1-x}Sr_xTiO_3$ thin films on nichrome substrate. The SEM micrographs of the surface morphology of $Ba_{1-x}Sr_xTiO_3$ thin films show that despite using an off-axis arrangement the deposited films were uniform due the rotation of the substrate. It is worth mentioning that the films do not present cracks or pinholes.

The EDS quantification was restricted to the Ba, Sr. Ti and O; the signals from Ni and Cr were not taken into account. Table II presents the atomic concentration of each element obtained for each sample. It can be seen that as the Sr concentration increased the Ba concentration decreased with the concentration of Ti and O remaining in a relation close to 1:3, showing clearly the dependence of the composition with the RF power applied.

Figure 2 shows the XRD diffractograms of the $Ba_{1-x}Sr_xTiO_3$ films, and the positions of the diffraction peaks associated to the BaTiO$_3$ [16] and cubic SrTiO$_3$, represented with dotted and dashed lines respectively. The diffrac-
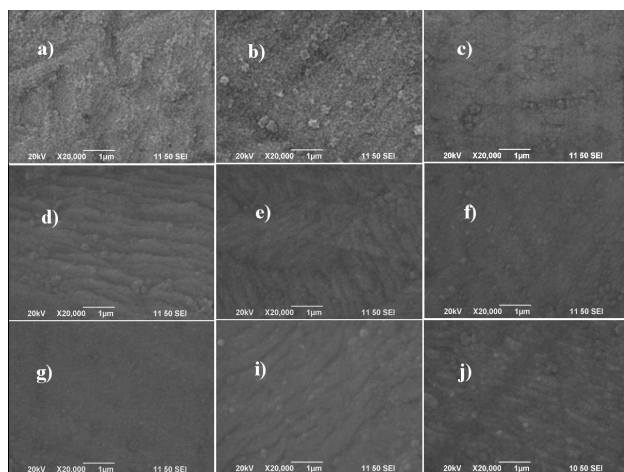
FIGURE 1. SEM micrographs showing the surface morphology for the Ba$_{1-x}$Sr$_x$TiO$_3$ thin films on nichrome substrate: a) BTO, b) BTO105, c) BTO90, d) BTO75, e) BTO60, f) BTO45, g) BTO30, i) BTO15 and j) STO sample.
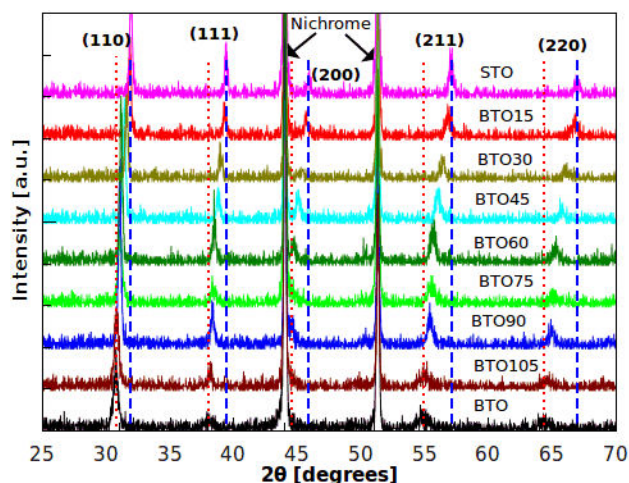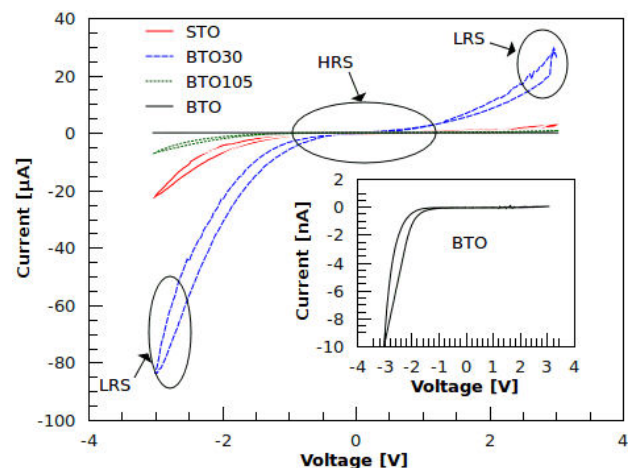

FIGURE 3. I-V curves of heterostructures fabricated with the STO, BTO, BTO30 and BTO105 thin films. The inset shows only the I-V curve of the heterostructure with BTO film in order to clarify the hysteresis effect.

FIGURE 2. XRD of the Ba$_{1-x}$Sr$_x$TiO$_3$ films studied. Dotted lines and dashed lines correspond to diffraction from the planes of BaTiO$_3$ and SrTiO$_3$, respectively.

tion peaks located at 44° and 51.3° are related to the nichrome. For x = 0 the peaks presented in the diffractogram are due to the diffraction from the (110), (111), (200), (211) and (220) planes of BaTiO$_3$ material (ICSD, Inorganically Crystal Structure Database and PDF, Power Diffraction File, card 310174) As the x parameter increases the BaTiO$_3$ peaks shift to higher angles. At x = 1, the peaks correspond to diffraction from the SrTiO$_3$ crystallographic planes (ICSD, Inorganically Crystal Structure Database and PDF, Power Diffraction File, card 350734) [1,8,17]. The shift of the diffraction peaks to higher angles as the RF power applied to the STO target increases reflects the decrease of the lattice parameter as the Sr content in the films increases. This behavior can be explained taking in account the difference of ionic ratio between Ba^{2+} (1.35 Å) and Sr^{2+} (1.18 Å). These results suggest that the lattice parameters of these films change due to the substitution of the Ba by the Sr. The difference on the

peaks positions of the cubic and tetragonal structure of BaTiO$_3$ are of the order of the experimental uncertainty of our measurements, therefore it is quite difficult to resolve the precise crystal structure of the films. To specify the crystal structure beyond any doubt it would be necessary to increase the signal to noise ratio of the XRD data and refine the structure by the Rietveld method. However there are some reports for Ba$_{1-x}$Sr$_x$TiO$_3$ for x=0 [16], x=0.33 [18], x= 0.408 [19] and x= 0.744 [20] in which the structure is reported as cubic.

To evaluate the influence of chemical composition of the BST thin films on the resistive switching behavior the $I–V$ curves of Al/Ba$_{1-x}$Sr$_x$TiO$_3$/nichrome heterostructures were obtained at room temperature under a voltage sweep: 0→+3V→0→-3V→0. The $I-V$ curves were recorded with a Keithley 2410 source meter unit; a current compliance of 1 mA was used and during the electrical measurements the bias voltage was applied to the top electrode while the bottom electrode was grounded. Taking advantage of the patterned Al electrodes, the I-V tests were conducted at various points for each sample. In Fig. 3 typical I-V curves for the STO, BTO30, BTO105 and BTO samples are shown. All as-grown heterostructures were in HRS, after sweeping the voltage from zero to positive values a small change in their resistivity is observed, for all of them except BTO30 sample, but they remained in the HRS. For the BTO30 heterostructure at a positive voltage value, a jump of current appeared and its resistance switched to the LRS. Sweeping again, the current dropped and the resistance went back to the HRS. All heterostructures are switched to the LRS by sweeping the voltage to negative values. However, the value of the current drained through the resistive cell depends on the chemical composition of the BST films.

In Fig. 3 only the LRS for the BTO30 sample is presented, but this behavior is observed for the whole set of samples. The inset in Fig. 3 is a zoom to the I-V curve of BTO sample that allows the observation of a hysteresis effect. The
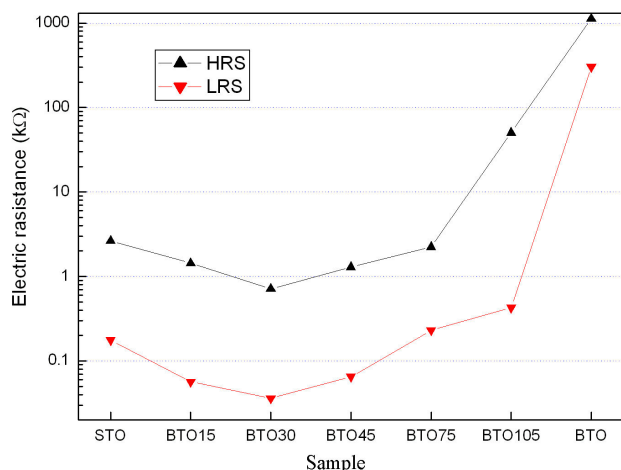
FIGURE 4. Electrical resistance of heterostructures as a function of the samples.

asymmetric behavior observed in the I-V curve was clearly observed for all samples, only the BTO30 film shows a resistive switching behavior in both voltage polarities with a clear hysteresis curve. This form of the I-V curves is commonly reported and it is attributed to the asymmetry of the contacts due to the use of different metal to form the bottom and the top contacts [21].

Figure 4 shows the resistance for all the samples calculated from I–V curves for LRS and HRS. Resistance in both the HRS and LRS varies non-linearly with the barium content on the films. As can be seen in Fig. 4, the increase in relative concentration of barium has the effect of reducing the electrical resistance with respect to that of the STO film, until values like those of BTO30 sample are reached. However, when the barium content is higher the electrical resistance gradually increases and reaches its maximum value for the BTO

sample. Then, an adequate value of the Ba/Sr ratio can be used to tune the electrical resistance of the films. In ReRAM cells an important parameter is the value of the difference of the resistance between the LRS and the HRS, the bigger is the better. For the set the samples studied the maximum difference in resistance between these two states is obtained for the BTO105 sample as can be seen in Fig. 4. However, the resistance values are large in comparison with those obtained for the heterostructures containing films with barium content less than the BTO105 sample, but it does not have a good hysteresis curve. On the other hand, it can be seen that the BTO30 sample shows the lowest values in resistance in the two states, in addition, to making the best hysteresis curve. This suggests that the composition of BTO30 sample allows obtaining the best behavior of resistive switching.

4. Conclusions

$Ba_{1-x}Sr_xTiO_3$ thin films with $0 \leq x \leq 1$ were obtained by off-axis rf co-sputtering, using $BaTiO_3$ and $SrTiO_3$ targets. The composition, as determined by the value of x, is controlled through the power applied to the targets. The electrical properties of the samples were changed by varying the Ba/Sr ratio. The results confirm that $Ba_{1-x}Sr_xTiO_3$ thin films are a suitable material for the development of ReRAM memories. The best resistance switching was obtained for the composition corresponding to the BTO30 sample.

Acknowledgements

1. A. Zapata-Navarro, A. Márquez-Herrera, M.P. Cruz-Jáuregui and M.L. Calzada, *Phys. Stat. Sol.* **2** (2005) 3673.

2. G.A. Hirata, L.L. López, and J. M. Siqueiros, *Sup. y Vac.* **9** (1999) 147.

3. L. Shi-jian, X. Chong-Yang, Z. Xiang-Bin, S. Ji-Qun, and Z. Bo-Fang, *Phys. Stat. Sol.* **194** (2002) 64.

4. V. Ruckenbauer *et al.*, *Appl. Phys. A* **78** (2004) 1049.

5. S.W. Kirchoefer *et al.*, *Micr. Opt. Tech. Lett.* **18** (1998) 169.

6. V.N. Keis, A.B. Kozyrev, M.L. Khazov, J. Sok, and J.S. Lee, *Elect. Lett.* **11** (1998) 3.

7. J.G. Cheng, J. Tang, J.H. Chu, and A.J. Zhang, *Appl. Phys. Lett.* **77** (2000) 1035.

8. S.U. Adikary and H.L.W. Chan, *Thin Solid Films* **424** (2003) 70.

9. C.B. Lee *et al.*, *Appl. Phys. Lett.* **93** (2008) 042115.

10. A. Márquez-Herrera, E. Hérnandez-Rodríguez, M.P. Cruz-Jauregui, M. Zapata-Torres and A. Zapara-Navarro, *Rev. Mex. Fis.* **56** (2010) 85.

11. T. Ishijima, K. Goto, N. Ohshima, K. Kinoshita, and H. Toyoda, *Jpn. J. Appl. Phys.* **48** (2009) 116004.

12. K. Tominaga, T. Kikuma, K. Kusaka, and T. Hanabusa, *Vacuum* **66** (2002) 279.

13. T.A. Jennings and W. McNeill, *Appl. Phys. Lett.* **12** (1968) 25.

14. A. Marquez-Herrera, A. Zapata-Navarro and Ma. De La Paz Cruz-Jauregui, *J. Of Mat. Sci.* (2005) 1.

15. E. Hernández-Rodríguez, A. Márquez-Herrera, M. Meléndez-Lira, and M. Zapata-Torres, *Mat. Sci. Eng. B* (2010) doi:10.1016/j.mseb.2010.05.017.

16. Moo-Chin Wanga, Fu-Yuan Hsiao, Chi-Shiung Hsi, and Nan-Chung Wu, *Journal of Crystal Growth* **246** (2002) 78.

17. Y. Xu, "*Ferroelectric Materials and their applications*". North Holland. *Elsevier Science Publishers* (B.V. New York.1991).

18. R.S. Liu *et al.*, *Materials Letters* **37** (1998) 285.

19. R. Varatharajan *et al.*, *Crystal Enginnereing* **3** (2000) 195.

20. J. Joseph, T.M. Vimala, J. Raju, and V.R.K. Murthy, *Journal of Physics D: Applied Physics* **32** (1999) 1049.

21. X. Cao, X. Li, W. Yu, X. Liu, and X. He, *Mat. Sci. Eng. B* **157** (2009) 36.